

Structure-Specific *N*-Glycoproteomics Characterization of NIST Monoclonal Antibody Reference Material 8671

Ming Bi, Bing Bai,* and Zhixin Tian*

Cite This: *J. Proteome Res.* 2022, 21, 1276–1284

Read Online

ACCESS |



Metrics & More



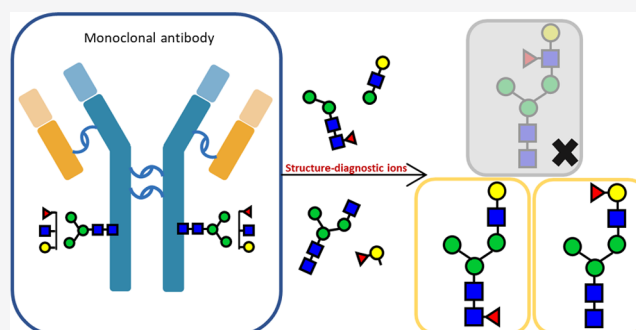
Article Recommendations



Supporting Information

ABSTRACT: The characteristics of monoclonal antibodies (mAbs) cohering various function effectors show great expectation in therapy. Glycosylation, one of the common post-translational modifications, deeply influences cohesion. It is necessary to grasp monosaccharide composition/sequence and glycan structures in mAbs. There has been comprehensive mass spectrometry characterization of *N*-glycosylation of mAbs, and monosaccharide compositions are deduced according to known biosynthetic rules. Our recently developed intact *N*-glycopeptide search engine GPSeeker has made structure-specific characterization of *N*-glycosylation possible with structure-diagnostic fragment ions from selective fragmentation of *N*-glycan moieties. Here, we report our structure-specific *N*-glycoproteomics characterization of NIST monoclonal antibody reference material 8671 using GPSeeker, and 59 *N*-glycan structures (including 16 pairs of isomers) are characterized.

KEYWORDS: monoclonal antibody, intact *N*-glycopeptide, GPSeeker, structure of *N*-linked glycan



monoclonal antibody reference material 8671 using GPSeeker, and 59 *N*-glycan structures (including 16 pairs of isomers) are characterized.

1. INTRODUCTION

The development of monoclonal antibodies (mAbs) has a history of about 50 years.¹ By 2021, up to 100 therapeutic mAbs have been approved and adopted for the treatment of various diseases including cancers.² Molecularly, mAbs are one of the γ -immunoglobulin isotypes, and every mAb molecule is composed of two heavy chains and two light chains.³ In terms of function, every mAb molecule has two distinct domains, i.e., the fragment of antigen-binding (Fab) domain and the fragment crystallizable (Fc) domain: the former recognizes and binds antigens, and the latter is responsible for recruiting effector molecules or cells. The co-play of these two domains leads to immune responses including antibody-dependent phagocytosis (ADPH),⁴ antibody-dependent cellular cytotoxicity (ADCC),⁵ and complement-dependent cytotoxicity (CDC).⁶

N-glycosylation on *N*-glycosite N297 in the Fc domain deeply influences stability, effector functions, ligand or cell binding, and immunogenicity of mAbs because of hydrophobic and hydrophilic interactions between sugar residues and amino acid residues.⁷ Microheterogeneity develops its importance in mAbs. For example, mAbs with terminal sialic acids have a longer half-life⁸ in the case of an asialoglycoprotein receptor and may influence the function of ADCC and CDC;^{9–11} on the other hand, mAbs with terminal mannose have a shorter half-life and weaker ADCC.¹² The biggest influence comes from core fucose in ADCC,¹³ which inhibits the effector, whereas the bisect GlcNAc has an opposite effect.¹⁴ Terminal galactose can increase CDC.¹⁵ α -Galactose and NeuGc may introduce

antidrug antibodies.¹⁶ By and large, for *N*-glycosylation on N297, both the terminal and core structures of the glycans have direct impact on the functions and properties of mAbs.

As one of the critical quality attributes (CQAs) of mAbs, structural analysis of mAb *N*-glycosylation is in demand.¹⁷ The detailed structures of modified *N*-glycans, including number of sialic acids, degree of mannosylation, terminal galactose, and core fucose, should be known.¹⁸ Therefore, new methods for accurate and sensitive analysis of mAb *N*-glycosylation should be developed. The National Institute of Standards and Technology (NIST) provides reference materials (RM) for promoting accuracy and metrological traceability of chemical measurements and validation of chemical measurement processes.¹⁹ NIST RM 8671, a humanized IgG with an *N*-glycosite in the Fc domain, is widely used as an mAb model for methods evaluation. There have been numerous efforts in interpreting the *N*-glycan structures of RM 8671. Dong et al.²⁰ built a spectral library with the assistance of two-dimensional reversed-phase liquid chromatography-tandem mass spectrometry (2D-RPLC-MS/MS) and identified 247 intact *N*-glycopeptides and 60 *N*-glycan compositions. Hilliard et al.²¹

Received: January 16, 2022

Published: March 29, 2022



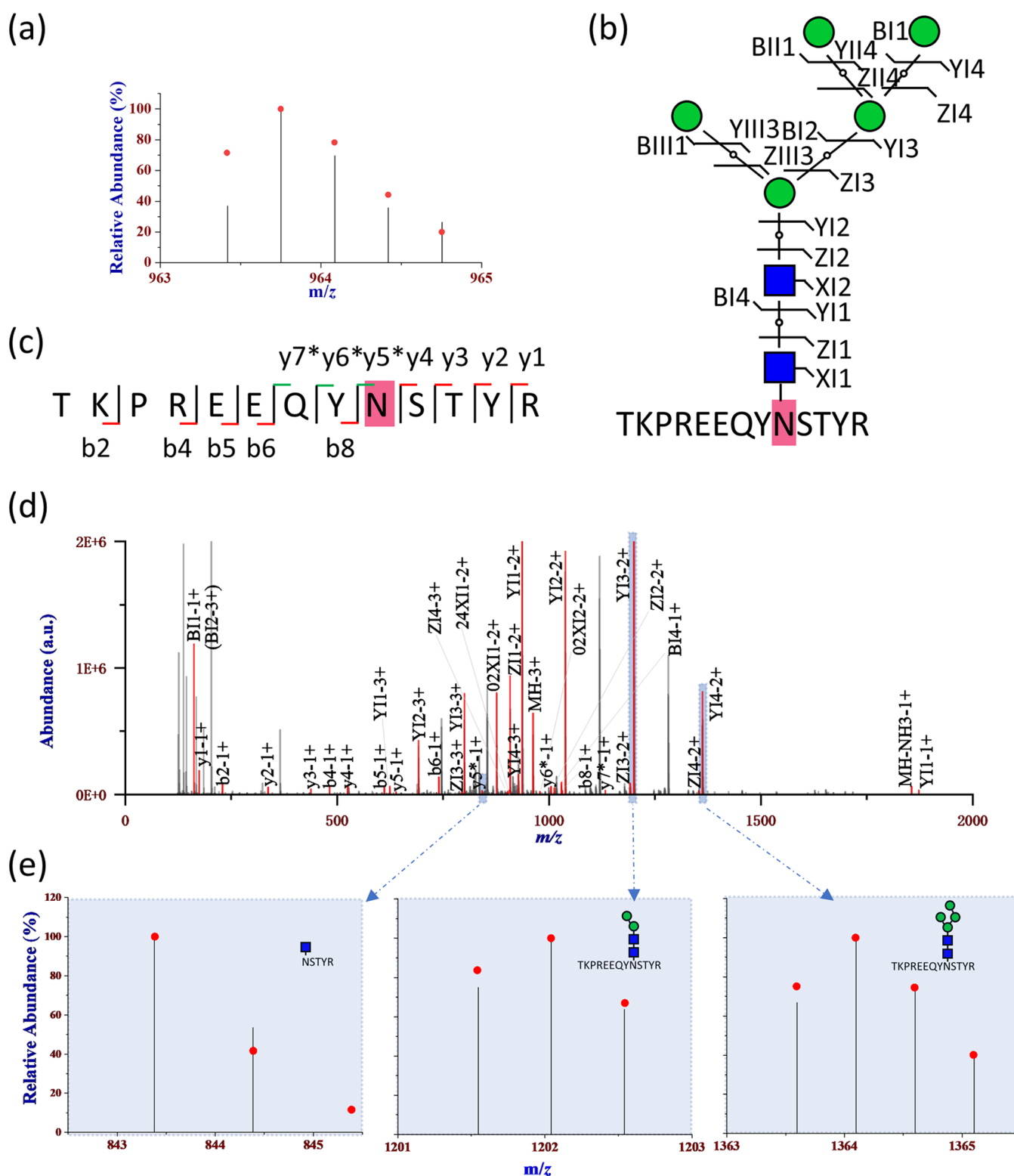


Figure 1. Site- and structure-specific identification of intact N-glycopeptide TKPREEQYNSTYR_N2H5F0S0 using site-determining and structure-diagnostic fragment ions from the peptide backbone and N-glycan moiety, respectively: (a) fingerprinting map of the experimental (bars) and theoretical (dots) isotopic envelope of the precursor ion, (b, c) graphical fragmentation maps of the N-glycan moiety and peptide backbone, (d) annotated MS/MS spectrum, and (e) isotopic envelop fingerprinting maps of representative GlcNAc-containing and structure-diagnostic fragment ions.

analyzed N-glycans of NIST 8671 (released by PNGase F) and confirmed 35 masses. The most up-to-date tandem MS study identified 48 monosaccharide compositions and confirmed 21 sequence structures.²² NIST recently organized a community-

wide study by sending the material to 76 laboratories worldwide, and up to 116 compositions are comprehensively characterized and 150 structures are generally represented based on biological inference without direct structural information.²³

Here, we report our structure-specific *N*-glycoproteomics characterization of RM 8671 with GPSeeker search of structure-diagnostic fragment ions from tandem mass spectra to distinguish different monosaccharide sequence structures from the same monosaccharide composition: 59 intact *N*-glycopeptides with distinct *N*-glycan structures including 16 pairs of structure isomers are identified. GPSeeker,²⁴ an intact *N*-glycopeptide search engine, was previously successfully used for structure-specific *N*-glycan characterization of recombinant COVID-19 S-protein,²⁵ as well as complex *N*-glycoproteomes from various sample types, e.g., urine,²⁶ cell,²⁷ and tissue.²⁸ Shen et al.²⁶ identified 2986 intact *N*-glycopeptides including 146 confirmed *N*-glycan structures in human urine. In the study of differential *N*-glycosylation of MCF-7/ADR cancer stem cells, Wang et al.²⁷ identified 546 *N*-glycopeptides with structure-diagnostic ions. Most recently, Lu²⁸ et al.²⁸ reported 1152 intact *N*-glycopeptide-modified structure isomers with structure-diagnostic ions in pancreatic cancer tissues.

2. MATERIALS AND METHODS

2.1. Reagents

NIST humanized IgG1k monoclonal antibody reference material (mAb RM) 8671, DL-dithiothreitol (DTT), iodoacetamide (IAA), acetonitrile (ACN), trifluoroacetic acid (TFA), and formic acid (FA) were purchased from Sigma-Aldrich (St. Louis). Urea, ammonium bicarbonate (ABC), and BCA Protein Assay Kit were bought from Sagon Biotech (Shanghai, China). Sequencing-grade modified trypsin was bought from Promega (Madison). Ultrapure water was produced onsite with a Millipore Simplicity System (Billerica, MA).

2.2. Sample Preparation of Intact *N*-Glycopeptides

NIST mAb RM 8671 (300 μ g) were denatured by 8 M urea, reduced by 20 mM DTT for 20 min at 55 °C, and alkylated with 20 mM IAA for 30 min in dark. Then, the residual IAA was reacted with 20 mM DTT for 30 min at room temperature. After 50 mM ABC dilution, 6 μ g of trypsin was added for digestion for 16 h at 37 °C. Home-made C18 (15 μ m, Jupiter, Phenomenex) SPE columns were used for desalting. Briefly, 1.5 mg of C18 was loaded into a 1 mL peptide tip and equilibrated with 80% ACN containing 0.1% TFA and subsequently 0.1% TFA. Then, the digestion solution was loaded into the column, and the loading process was repeated four more times. The column was then washed with 800 μ L of 0.1% TFA, and peptides were eluted twice with 50% ACN containing 0.1% TFA and 80% ACN containing 5% TFA, respectively. The eluants were combined and dried in a SpeedVac (Thermo Fisher Scientific, USA).

Intact glycopeptides were enriched from the desalting peptides with a ZIC-HILIC (5 μ m, SeQuant, Merck) SPE column. Peptides were dissolved in 80% ACN containing 5% TFA solution. After the ZIC-HILIC SPE column was equilibrated twice with 0.1% TFA and 5% TFA in 80% ACN, respectively, the peptide solution was loaded five times. The column was then washed with 800 μ L of 80% ACN with 5% TFA, and intact *N*-glycopeptides were eluted twice with 0.1% TFA and 50 mM ABC, respectively. The eluants were combined and dried in the SpeedVac and resuspended in 40 μ L of H₂O for downstream LC-MS/MS analysis.

2.3. RPLC-MS/MS

RPLC-MS/MS analysis of the enriched intact *N*-glycopeptides of RM 8671 was carried out on Dionex Ultimate 3000 RSLC coupled to nano-ESI Q Exactive MS (Thermo Fisher Scientific,

San Jose, CA). The trap column (200 id, 7 cm long) and analytical column (75 μ m id, 70 cm long) were both packed in-house with C18 (5 μ m, 300 Å, Jupiter, Phenomenex). Buffer A was 99.8% H₂O with 0.2% FA, and Buffer B was 95% ACN with 0.2% FA. The loading and elution flow rates were 3.0 and 0.3 μ L/min, respectively. The multistep gradient settings were as follows: 2% buffer B, 20 min; 2–40% buffer B, 190 min; 40–95% buffer B, 10 min; 95% buffer B, 10 min; 95–2% buffer B, 10 min; and 2% buffer B, 10 min.

The spray voltage, ion transfer tube temperature, and S-lens RF level were 2.8 kV, 250 °C, and 50%, respectively. MS spectra were acquired with the parameters of *m/z* 700–2000, mass resolution 70 000, automatic gain control (AGC) target 2e5, and maximum injection time 200 ms. MS/MS spectra were acquired in the DDA mode for top 20 ions with mass resolution 17 500, AGC target 5e5, maximum injection time 250 ms, isolation windows 3 *m/z*, higher energy collision dissociation with normalized collision energies 20/30/30%,²⁹ and dynamic exclusion 20 s.

2.4. Database Search and Identification of Intact *N*-Glycopeptides

Intact *N*-glycopeptides were searched and identified by GPSeeker with maximal missed cleavage of one and minimal peptide length of 6; the isotopic peak *m/z* deviation (IPMD), isotopic peak abundance cutoff (IPACO), and isotopic peak abundance deviation (IPAD) for both the precursor and fragment ions were 20 ppm, 40, and 50%, respectively. The theoretical *N*-glycan library contained 108 921 monosaccharide sequence structures built according to the retrosynthetic strategy and currently known biosynthesis rules.³⁰ The theoretical fragment ions of every *N*-glycan include ^{*m,n*}A (bond number *m* = 0, 1, 2, 3, 4; bond number *n* = 1, 2, 3, 4, 5; *m* < *n*), B, C, ^{*m,n*}X (*m* = 0, 1, 2, 3, 4; *n* = 1, 2, 3, 4, 5; *m* < *n*), Y, Z, and internal ions (limited to Y-^{0,2}Al, Y-^{2,4}Al, Z-^{0,2}Al, Z-^{2,4}Al; Al ions come from either Y in the core structure; I is the number one branch). In the case of identification of one monosaccharide composition corresponding to multiple sequence structures, GPSeeker automatically searches for experimental structure-diagnostic fragment ions, where a distinct structure can be confirmed with no less than one structure-diagnostic fragment ion.

In addition to GPSeeker, intact *N*-glycopeptide search engine pGlyco 3.0³¹ was also adopted for monosaccharide composition-level search with precursor and fragment mass tolerance values of 10 and 20 ppm, respectively.

3. RESULTS AND DISCUSSION

In search and identification of an intact *N*-glycopeptide by GPSeeker, the peptide backbone is first identified from the Y1 ion and then the *N*-glycan moiety and intact *N*-glycopeptide. Taking the intact *N*-glycopeptide TKPREEQYN-STYR_N2H5F0S0 as an example, there is a good match between the theoretical (dots) and experimental (bars) isotopic envelopes of the precursor ion (Figure 1a); efficient fragmentation of both the peptide backbone and the *N*-glycan moiety brings not only confident identification (Figure 1c/d,b) but also confident *N*-glycosite localization and monosaccharide sequence structure distinction. GlcNAc-containing fragment ions y5* (*m/z* = 843.38), y6* (*m/z* = 1006.45), and y7* (*m/z* = 1134.51) each can independently localize the *N*-glycosite; unique fragment ions from the *N*-glycan moiety YI3-2 + (*m/z* =

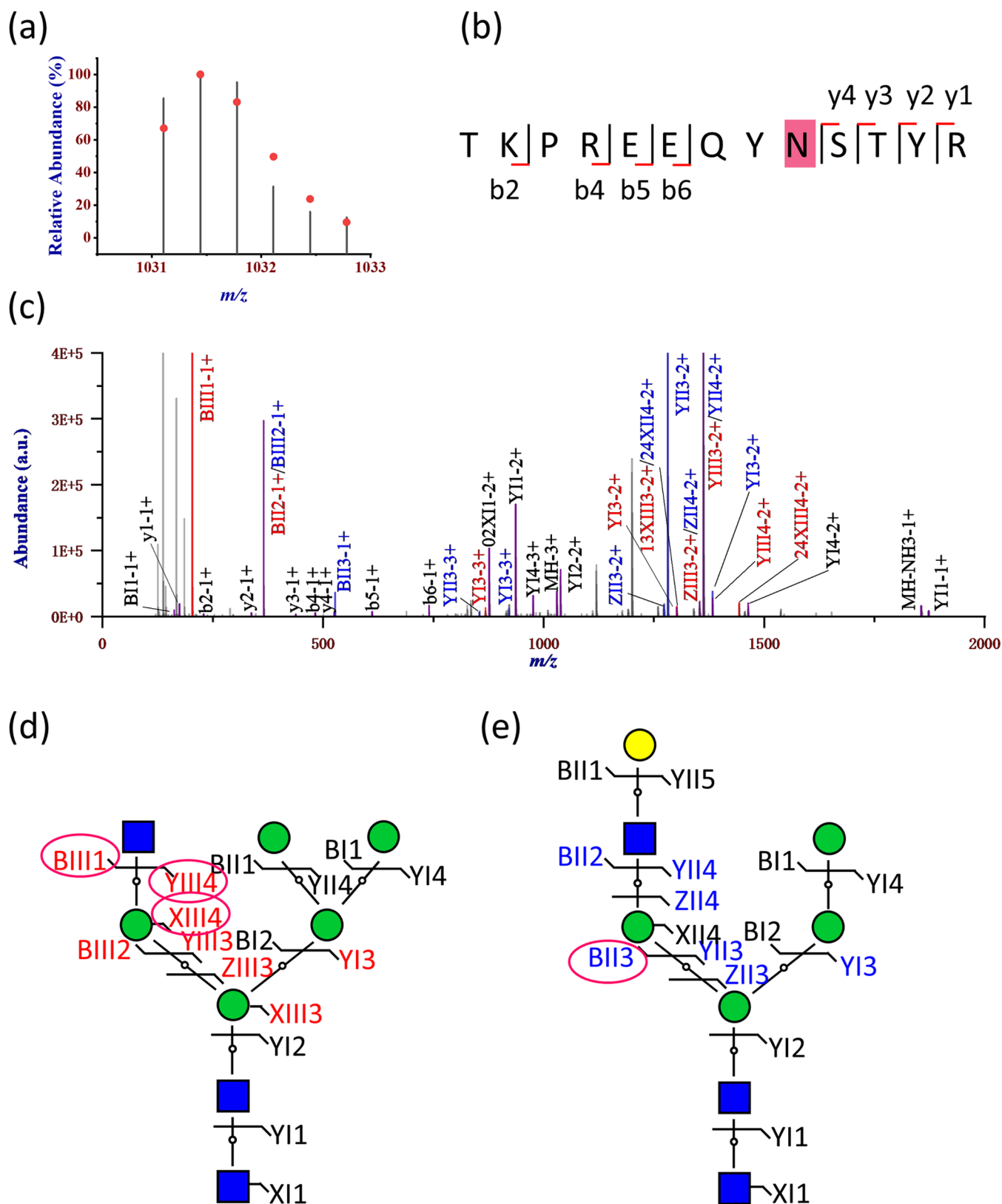


Figure 2. Identification of monosaccharide sequence isomers of intact *N*-glycopeptide TKPREEQYNSTYR_{N3H5F0S0} using *s* structure-diagnostic fragment ions from the *N*-glycan moiety: (a) fingerprinting map of the experimental (bars) and theoretical (dots) isotopic envelope of the precursor ion, (b, d, e) graphical fragmentation maps of the peptide backbone and the two *N*-glycan sequence isomers, and (c) annotated MS/MS spectrum.

1202.04) and Y14-2 + ($m/z = 1364.10$) each can independently distinguish this structure from all of the other sequence isomers.

With the aforementioned search and identification procedure, 188 intact *N*-glycopeptides were identified with monosaccharide sequence structures. With structure-diagnostic fragment ions, 59

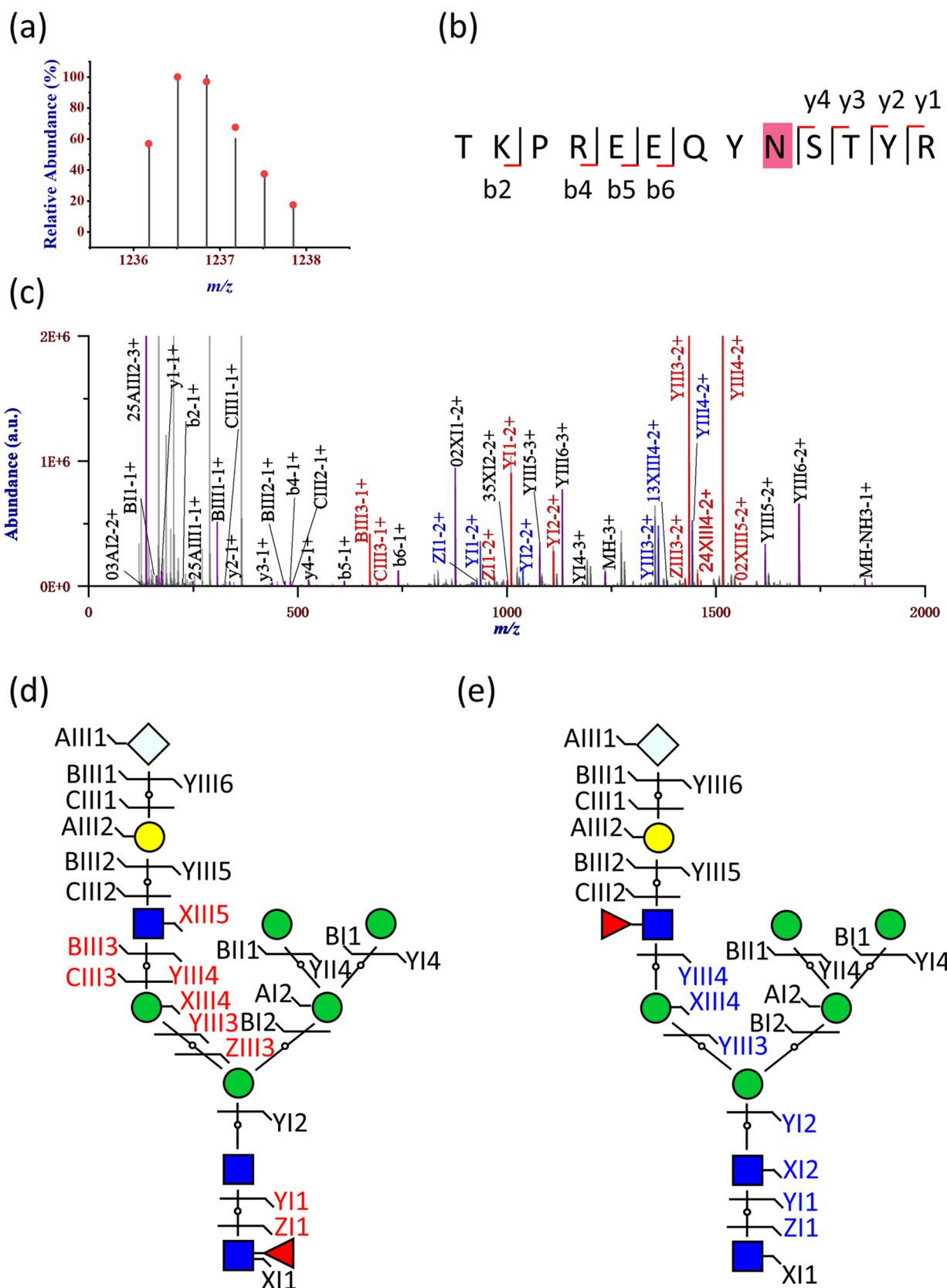


Figure 3. Identification of fucose position isomers of intact N-glycopeptide TKPREEQYNSTYR_N3H6F1S0G1 using structure-diagnostic fragment ions from the N-glycan moiety: (a) fingerprinting map of the experimental (bars) and theoretical (dots) isotopic envelope of the precursor ion, (b, d, e) graphical fragmentation maps of the peptide backbone and the two N-glycan sequence isomers, and (c) annotated MS/MS spectrum.

structures (from 38 compositions) including 16 pairs were experimentally confirmed and distinguished from their sequence

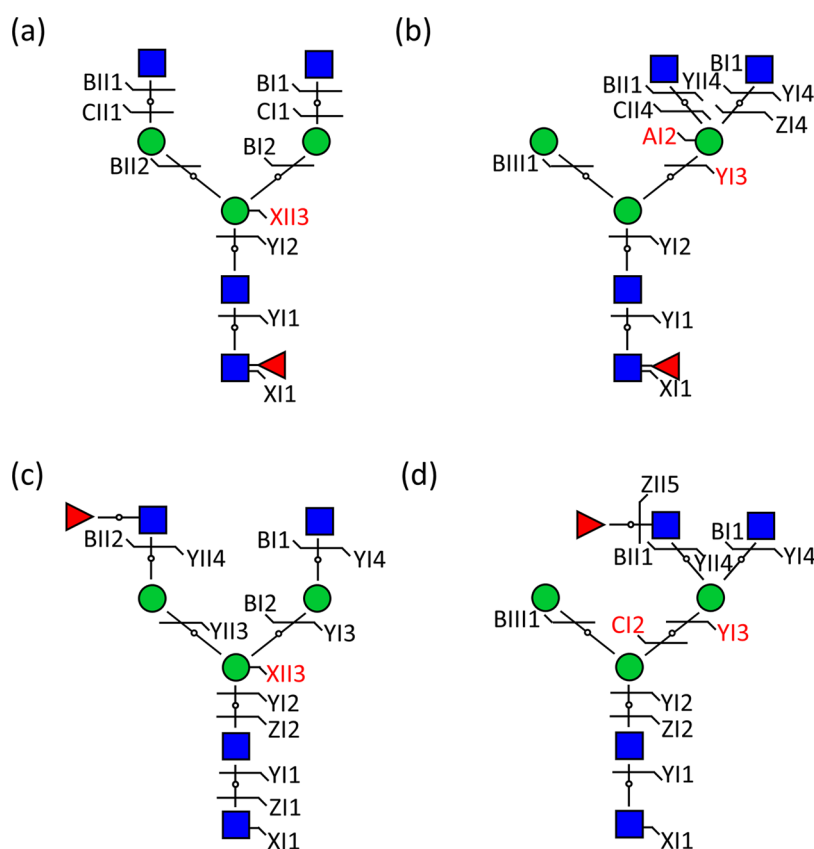


Figure 4. Graphical fragmentation maps of combinatorial monosaccharide sequence and fucose position isomers of *N*-glycan N4H3F1S0: (a–d) one (XII3), two (AI2, YI3), one (XII3), and two (CI2 and YI3) structure-diagnostic fragment ions, respectively.

isomers. The detailed information of composition, structure, and structure-diagnostic ions of the 59 confirmed structures is provided in Table S1.

Among the 16 paired isomers, 11 pairs are sequence isomers. For example, the monosaccharide composition in the intact *N*-glycopeptide TKPREEQYNSTYR_N3H5F0S0 has four theoretical monosaccharide sequence structures (01Y41Y41M-(31M)(41Y)61M31M21M, 01Y41Y41M(31M)(41Y)61M-(31M)61M, 01Y41Y41M(31M41Y41L)61M61M, 01Y41Y41M(31M41Y)61M(31M)61M) in our human theoretical *N*-glycan DB. In the MS/MS spectrum, BIII1-1 + (m/z = 204.09) and YIII4-2 + (m/z = 1445.12) indicated the existence of a structure with a terminal GlcNAc, and the *N*-glycan structure has three antennas (Figure 2d). In addition, the intraring fragment ion $^{1,3}\text{XIII3-2} +$ (m/z = 1304.08) indicates that the branch containing GlcNAc is connected to the third C atom of the core mannose. The fragment ion BII3-1 + (m/z = 528.18) indicated the existence of a structure with an antenna composed of two hexose and one GlcNAc (Figure 2e).

In addition to sequence isomers, nine pairs of fucose position isomers, a special type of sequence isomers, are also identified in this study. As an example of TKPREEQYNSTYR_N3H6F1S0G1, the core and branch isomers were distinguished from each other with nine and seven structure-diagnostic fragment ions, respectively (Figure 3). For example, fragment ions BIII3-1 + (m/z = 308.10) and YI1-2 + (m/z = 1011.48) as well as ZI1-2 + (m/z = 1002.47) indirectly and directly localize the fucose on the core (Figure 3d). On the other hand, the absence of fucose in the doubly charged YI1 (m/z = 937.95) and ZI1 (m/z = 928.94) ions gives the evidence of the branch fucose structure (Figure 3e).

Sequence and position isomers may exist simultaneously for a single monosaccharide composition, and four structure isomers appear altogether. For example, for N4H3F1S0, four distinct structures 01Y(61F)41Y41M(31M21Y)61M21Y, 01Y(61F)-41Y41M(31M)61M(21Y)61Y, 01Y41Y41M(31M21Y31F)-61M21Y, and 01Y41Y41M(31M)61M(21Y31F)61Y are confirmed with one ($^{2,3}\text{XII3}$ (m/z = 868.07, z = 3)), two ($^{0,1}\text{AI2}$ (m/z = 324.13, z = 1) and YI3 (m/z = 1085.53, z = 4)), one ($^{1,4}\text{XII3}$ (m/z = 1258.57, z = 2)), and two (CI2 (m/z = 367.14, z = 2) and YI3 (m/z = 801.70, z = 3)) structure-diagnostic ions (Figure 4).

With the special bisecting structure, GlcNAc position isomers also exist where a GlcNAc can be either on one of the branches or at the bisecting position. For composition N5H4F0S1, two such structural isomers (01Y41Y41M(31M(21Y)41Y)-61M21Y41L32S, 01Y41Y41M(31M)(41Y)61M(21Y41L32S)-61Y) were observed (Table S1).

The relative abundance of the identified *N*-glycan structures of RM 8671 was quantified with their precursor abundance in MS spectra, where the experimental abundance of the top 3 highest isotopic peaks was summed.

The relative abundance of different intact *N*-glycopeptides is shown in Figure S2, and the dominant compositions are N4H4F1S0, N4H3F1S0, N3H4F1S0, and N3H3F1S0. Among the 50 compositions identified, 28 contain fucoses counting for 91.51% relative abundance, 20 contain terminal sialic acids counting for 8.23% relative abundance, and 11 contain both fucoses and sialic acids, counting for 6% relative abundance (Figure S1b). In the latest paper analyzing the same mAb, 48 glycan compositions were identified; among these glycan compositions, the most abundant ones are N4H3F1S0

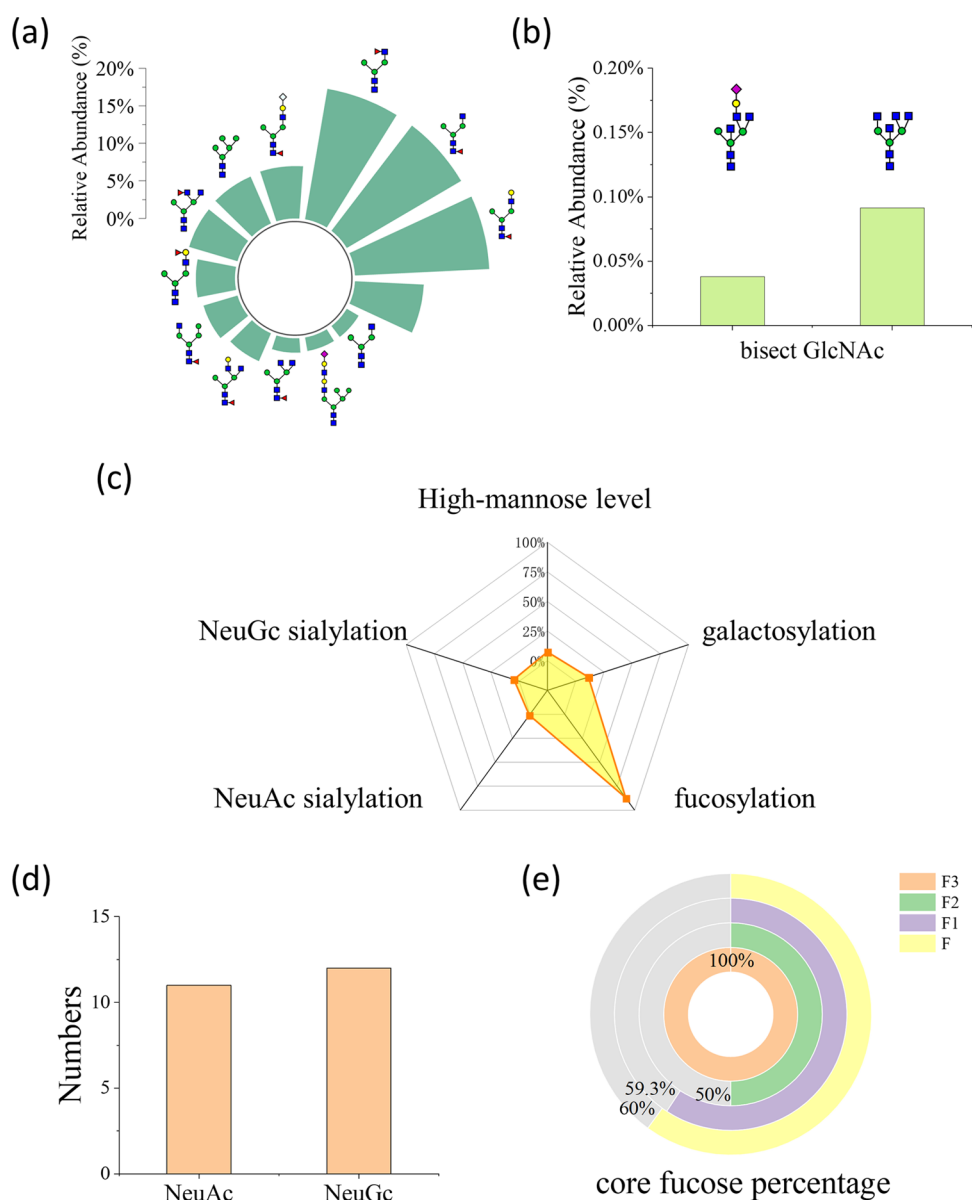


Figure 5. Quantitation of intact *N*-glycopeptides of 8671 with *N*-glycan structures confirmed in this study: (a) top 12 highest abundance of *N*-glycan structures, (b) relative abundance of two glycan structures with the bisecting GlcNAc, (c) frequency distribution of different types of *N*-glycosylation, (d) numbers of intact *N*-glycopeptides with different sialic acids of NeuAc and NeuGc, and (e) percentage of core fucosylation of *N*-glycans with different fucose stoichiometries.

(38.35%) and N3H4F1S0 (34.73%),²² consistent with our results.

Among the 59 *N*-glycan structures of RM 8671 identified in this study, the top 3 most abundant structures are N3H4F1S0 (18%, with a terminal galactose and a core fucose), N3H3F1S0 (18%, with a core fucose), and N3F3F1S0 (18%, with a branch fucose) (Figure 5a). In addition to the *N*-glycan structures listed in Figure 5a, the relative abundance of each of the other 47 structures was lower than 1%. The abundance of all of the 59 structures was summarized, and their relative abundance was calculated according to the previously reported method²³ (Figure 5c). High mannose level is the sum of relative abundance of all high-mannose *N*-glycans (7%). Galactosylation is the sum of the product of relative abundance and the galactosylation factor for all glycans with terminal galactose where the factor is the fraction of antennae that are galactosylated (1%). In the same way, NeuAc sialylation and

NeuGc sialylation are 1 and 5%, respectively. The relative abundance of NeuGc is over 5-fold that of NeuAc, but the numbers of glycan structures containing NeuAc and NeuGc are almost the same (Figure 5d). Fucosylation is the main glycosylation in RM 8671 (87%), and the number of core fucosylation constitutes 60% (Figure 5e). The *N*-glycans modified with one, two, or three fucoses have 59, 50, and 100% core fucosylation, respectively. Bisecting *N*-glycans are rarely identified because these are always coeluted with isomers or have low intensities. Although the relative abundances are lower than 0.1%, two bisecting GlcNAc structures are identified in this paper (Figure 5b).

In addition to structure-specific search using GPSeeker, complementary composition-specific search using pGlyco 3.0 was carried out, and 75 intact *N*-glycopeptides with distinct monosaccharide compositions were identified; there are 38 common compositions between the two search engines. For *N*-

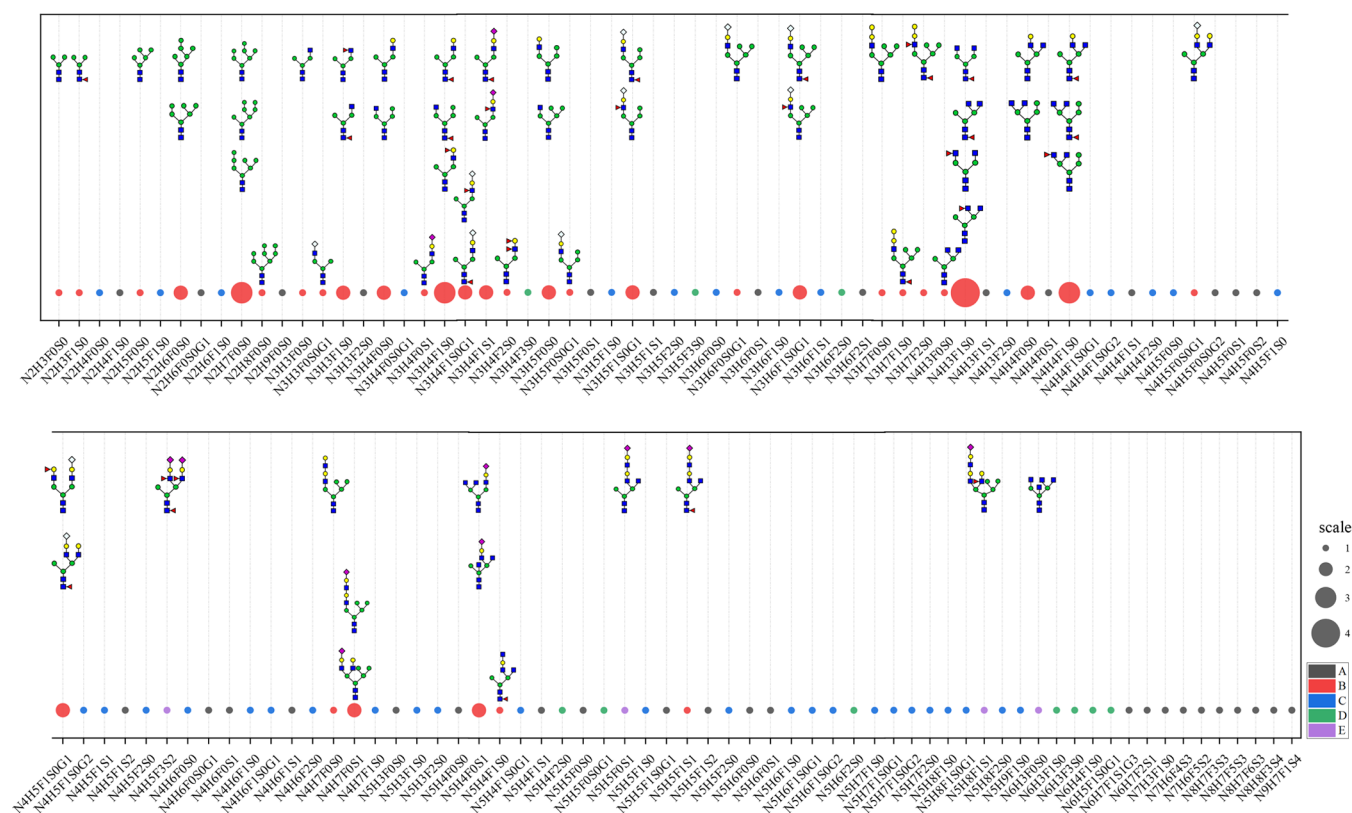


Figure 6. Overall site- and structure-specific *N*-glycosylation identification of RM 8761. Every glycan composition is represented with a circle: blue ones mean common identification in both this study and the interlaboratory study; black ones mean unique in the interlaboratory study; red ones mean structures identified; green ones mean unique in this study; and purple ones mean structure IDs in this study. The size of the circles reflects the number of structures.

glycan structures, this study and the NIST interlaboratory study share 28 (Figure S3).

Among the 87 intact *N*-glycopeptides with common five-membered trimannosyl chitoiose core structures, 73 are also reported in the recent interlaboratory study (Figure 6), while there are 34 common monosaccharide compositions, each of which has 1–4 sequence structures. Fourteen compositions (N3H4F3S0, N3H5F3S0, N3H6F2S0, N4H5F3S2, N5H4F2S0, N5H5F0S0G1, N5H5F0S1, N5H6F2S0, N5H8F1S1, N6H3F0S0, N6H3F1S0, N6H3F3S0, N6H4F1S0, and N6H5F1S0G1) were uniquely identified in this study, where distinct sequence structures were identified for four compositions (N4H5F3S2, N5H5F0S1, N5H8F1S1, and N6H3F0S0).

4. CONCLUSIONS

Monosaccharide sequence structures of *N*-glycosylation of NIST monoclonal antibody reference material 8671 were characterized with structure-specific *N*-glycoproteomics using structure-diagnostic fragment ions, which are automatically searched and identified by the intact *N*-glycopeptide search engine GPSeeker. Fifty-nine *N*-glycan structures (including 16 pairs of isomers) were distinguished from their sequence isomers with no less than one structure-diagnostic fragment ion. The most abundant monosaccharide composition is N4H4F1S0, and three out of the 15 putative sequence structures in our *N*-glycan theoretical database were identified.

With the commercialization and widely available mass spectrometers with efficient dissociation methods, structure-diagnostic fragment ions to distinguish monosaccharide

sequence isomers can be obtained efficiently; utilizing this advancement, intact *N*-glycopeptide search engine GPSeeker will find wide application in structure-specific *N*-glycosylation characterization of mAbs.

■ ASSOCIATED CONTENT

Supporting Information

The Supporting Information is available free of charge at <https://pubs.acs.org/doi/10.1021/acs.jproteome.2c00027>.

Identification and quantification results of intact *N*-glycopeptides: (a) number of identified identifications, putative structures, defined structures, and the corresponding composition numbers, (b) number and relative abundance of intact *N*-glycopeptide-modified fucose, sialic acid, and both (Figure S1); relative abundance distribution of glycans in all intact *N*-glycopeptides (Figure S2); overlap between the putative *N*-glycan structures reported in the NIST interlaboratory and the *N*-glycan structures confirmed with structure-diagnostic fragment ions reported in this study (Figure S3); and list of identified glycans with structure-diagnostic ions (Table S1) (PDF)

Accession Codes

The raw datasets are deposited to ProteomeXchange and can be reached with the submission reference number 1-20220314-150470.

■ AUTHOR INFORMATION

Corresponding Authors

Bing Bai – Department of Laboratory Medicine, Center of Precision Medicine, Nanjing Drum Tower Hospital, the Affiliated Hospital of Nanjing University Medical School, Nanjing, Jiangsu 210008, China; Email: bing.bai@nju.edu.cn

Zhixin Tian – School of Chemical Science & Engineering, Tongji University, Shanghai 200092, China; orcid.org/0000-0002-2877-8282; Email: zhixintian@tongji.edu.cn

Author

Ming Bi – School of Chemical Science & Engineering, Tongji University, Shanghai 200092, China

Complete contact information is available at:

<https://pubs.acs.org/10.1021/acs.jproteome.2c00027>

Notes

The authors declare no competing financial interest.

■ ACKNOWLEDGMENTS

This research was financially supported by the National Science Foundation of China (22074105) and the Shanghai Science and Technology Commission (14DZ2261100).

■ REFERENCES

- (1) Buss, N.; Henderson, S. J.; McFarlane, M.; et al. Monoclonal antibody therapeutics: history and future. *Curr. Opin. Pharmacol.* **2012**, *12*, 615–622.
- (2) Mullard, A. FDA approves 100th monoclonal antibody product. *Nat. Rev. Drug Discovery* **2021**, *20*, 491–495.
- (3) Vidarsson, G.; Dekkers, G.; Rispens, T. IgG subclasses and allotypes: from structure to effector functions. *Front. Immunol.* **2014**, *5*, No. 520.
- (4) Tay, M. Z.; Wiehe, K.; Pollara, J. Antibody-Dependent Cellular Phagocytosis in Antiviral Immune Responses. *Front. Immunol.* **2019**, *10*, No. 332.
- (5) Zhu, C.; Song, Z. L.; Wang, A. L.; et al. Isatuximab Acts Through Fc-Dependent, Independent, and Direct Pathways to Kill Multiple Myeloma Cells. *Front. Immunol.* **2020**, *11*, No. 1771.
- (6) Al-Youssef, N. L.; Ghobadloo, S. M.; Berezovski, M. V. Inhibition of complement dependent cytotoxicity by anti-CD20 aptamers. *RSC Adv.* **2016**, *6*, 12426–12429.
- (7) Raju, T. S. Terminal sugars of Fc glycans influence antibody effector functions of IgGs. *Curr. Opin. Immunol.* **2008**, *20*, 471–478.
- (8) Chen, X. Y.; Liu, Y. D.; Flynn, G. C. The effect of Fc glycan forms on human IgG2 antibody clearance in humans. *Glycobiology* **2009**, *19*, 240–249.
- (9) Quast, I.; Keller, C. W.; Maurer, M. A.; et al. Sialylation of IgG Fc domain impairs complement-dependent cytotoxicity. *J. Clin. Invest.* **2015**, *125*, 4160–4170.
- (10) Branstetter, E.; Duff, R. J.; Kuhns, S.; et al. Fc glycan sialylation of biotherapeutic monoclonal antibodies has limited impact on antibody-dependent cellular cytotoxicity. *FEBS Open Bio* **2021**, *11*, 2943–2949.
- (11) Thomann, M.; Malik, S.; Kuhne, F.; et al. Effects of sialic acid linkage on antibody-fragment crystallizable receptor binding and antibody dependent cytotoxicity depend on levels of fucosylation/bisecting. *Bioanalysis* **2019**, *11*, 1437–1449.
- (12) Mastrangeli, R.; Audino, M. C.; Palinsky, W.; et al. The Formidable Challenge of Controlling High Mannose-Type N-Glycans in Therapeutic mAbs. *Trends Biotechnol.* **2020**, *38*, 1154–1168.
- (13) Niwa, R.; Hatanaka, S.; Shoji-Hosaka, E.; et al. Enhancement of the antibody-dependent cellular cytotoxicity of low-fucose IgG1 is independent of Fc gamma RIIIa functional polymorphism. *Clin. Cancer Res.* **2004**, *10*, 6248–6255.
- (14) Hodoniczky, J.; Zheng, Y. Z.; James, D. C. Control of recombinant monoclonal antibody effector functions by Fc N-glycan remodeling in vitro. *Biotechnol. Prog.* **2005**, *21*, 1644–1652.
- (15) Bheemareddy, B. R.; Pulipeta, M.; Iyer, P.; et al. Effect of the total galactose content on complement-dependent cytotoxicity of the therapeutic anti-CD20 IgG1 antibodies under temperature stress conditions. *J. Carbohydr. Chem.* **2019**, *38*, 1–19.
- (16) Yehuda, S.; Padler-Karavani, V. Glycosylated Biotherapeutics: Immunological Effects of N-Glycolylneuraminic Acid. *Front. Immunol.* **2020**, *11*, No. 21.
- (17) Reusch, D.; Tejada, M. L. Fc glycans of therapeutic antibodies as critical quality attributes. *Glycobiology* **2015**, *25*, 1325–1334.
- (18) Uçaktürk, E. Analysis of glycoforms on the glycosylation site and the glycans in monoclonal antibody biopharmaceuticals. *J. Sep. Sci.* **2012**, *35*, 341–350.
- (19) Choquette, S. J.; Duewer, D. L.; Sharpless, K. E. NIST Reference Materials: Utility and Future. *Annual Review of Analytical Chemistry*; **2020**; Vol. 13, pp 453–474.
- (20) Dong, Q.; Yan, X. J.; Liang, Y. X.; et al. IN-Depth Characterization and Spectral Library Building of Glycopeptides in the Tryptic Digest of a Monoclonal Antibody Using 1D and 2D LC-MS/MS. *J. Proteome Res.* **2016**, *15*, 1472–1486.
- (21) Hilliard, M.; Alley, W. R.; McManus, C. A.; et al. Glycan characterization of the NIST RM monoclonal antibody using a total analytical solution: From sample preparation to data analysis. *mAbs* **2017**, *9*, 1349–1359.
- (22) Zhao, J. F.; Peng, W. J.; Dong, X.; et al. Analysis of NIST Monoclonal Antibody Reference Material Glycosylation Using the LC-MS/MS-Based Glycoproteomic Approach. *J. Proteome Res.* **2021**, *20*, 818–830.
- (23) De Leoz, M. L. A.; Duewer, D. L.; Fung, A.; et al. NIST Interlaboratory Study on Glycosylation Analysis of Monoclonal Antibodies: Comparison of Results from Diverse Analytical Methods. *Mol. Cell. Proteomics* **2020**, *19*, 11–30.
- (24) Xiao, K. J.; Tian, Z. X. GPSeeker Enables Quantitative Structural N-Glycoproteomics for Site- and Structure-Specific Characterization of Differentially Expressed N-Glycosylation in Hepatocellular Carcinoma. *J. Proteome Res.* **2019**, *18*, 2885–2895.
- (25) Yang, J.; Wang, W.; Chen, Z.; et al. A vaccine targeting the RBD of the S protein of SARS-CoV-2 induces protective immunity. *Nature* **2020**, *586*, 572–577.
- (26) Shen, Y.; Xiao, K.; Tian, Z. Site- and structure-specific characterization of the human urinary N-glycoproteome with site-determining and structure-diagnostic product ions. *Rapid Commun. Mass Spectrom.* **2021**, *35*, No. e8952.
- (27) Wang, Y.; Xu, F.; Chen, Y.; et al. A quantitative N-glycoproteomics study of cell-surface N-glycoprotein markers of MCF-7/ADR cancer stem cells. *Anal. Bioanal. Chem.* **2020**, *412*, 2423–2432.
- (28) Lu, H.; Xiao, K.; Tian, Z. Benchmark of site- and structure-specific quantitative tissue N-glycoproteomics for discovery of potential N-glycoprotein markers: a case study of pancreatic cancer. *Glycoconjugate J.* **2021**, *38*, 213–231.
- (29) Wang, Y.; Tian, Z. X. New Energy Setup Strategy for Intact N-Glycopeptides Characterization Using Higher-Energy Collisional Dissociation. *J. Am. Soc. Mass Spectrom.* **2020**, *31*, 651–657.
- (30) Xiao, K.; Wang, Y.; Shen, Y.; et al. Large-scale identification and visualization of N-glycans with primary structures using GlySeeker. *Rapid Commun. Mass Spectrom.* **2018**, *32*, 142–148.
- (31) Zeng, W. F.; Cao, W. Q.; Liu, M. Q.; et al. Precise, fast and comprehensive analysis of intact glycopeptides and modified glycans with pGlyco3. *Nat. Methods* **2021**, *18*, 1515–1523.